Adaptation of Dynamics in Default Mode Network Depending on Mental States: the One-to-many dynamic functional connectivity analysis with fMRI

Adaptation in dynamics of local brain network

Garam Jeong[1] and Marco Paolini[2]

[1]Institute of Medical Psychology, Ludwig Maximilian University of Munich
[2]Department of Radiology, University Hospital, Ludwig Maximilian University of Munich

Keywords

One-to-many dynamic functional connectivity, Default mode network, episodic memory retrieval, resting state, fMRI

Abstract

We suggest a novel analysis method called the one-to-many dynamic functional connectivity analysis to detect the adaptation of dynamics in a local brain network depending on mental states with a single case study. We collected fMRI BOLD signals from a blind subject whom with advanced ability in episodic memory retrieval while the subject was resting and retrieving a morning routine which is a type of autobiographical episodic memory. The default mode network is known for its high activation in these mental states. By applying the principal components analysis to the partial correlations of a brain region in the default mode network, which are correlations of the brain region to the rest of the network, we compared how congruent first or second principal components of the partial correlations of the brain region the default mode network in the two mental states. Our results showed that the adaption of the dynamics in the default mode network in the two mental states could be well depicted when the partial correlations of the posterior cingulate cortex are considered. Specifically, the correlation of the posterior cingulate cortex and the right parahippocampal cortex contributed mostly to the adaptation of the partial correlations of the posterior cingulate cortex for this single subject case.

1 Introduction

For the last few decades, research on human brains has found that some brain regions are highly active when the brain is resting without performing external tasks [23, 28]. These brain regions include roughly the posterior medial and the inferior lateral part of the parietal lobe and the medial prefrontal cortex. Also, functional connectivity analysis of the brain regions found that their activities are distinctly correlated when the brain is resting [10, 23, 53]. Because of these reasons, the set of brain regions was named the default mode network (DMN). The function of the DMN is an ongoing research topic. Meta-analysis revealed that the DMN is highly active not only during a resting state but also during an episodic memory retrieval state, an episodic future thinking state, a theory of mind state, or a navigation state [63, 62]. All these mental states construct internally mental imagery and focus on the imagery.

One of the suggested functions of the DMN regarding the commonalities between different brain states is “self-projection” [7, 12, 20]. Self-projection explains that the DMN processes the frame of reference of cognition consisting of subjective experiences. Hence, these cognitive activities happen internally regardless of sensory inputs from outside. For example, one can listen to a bird song without subjective experiences by self-projection. However, retrieving memory related to the bird song requires self-projection. Another interesting suggestion for the possible function of the DMN is “scene construction” [31]. The previously mentioned mental states in meta-analysis commonly require mental imagery of scenes. Sensory imageries from memory are ingredients to form and maintain such scenes. The two suggestions, self-projection and scene construction, stress two pivotal aspects of the mental states. One is the differentiation from perceptions generated with spontaneous sensory inputs, and the other is the creation of a coherent form of mental imagery. Taking it into account, the DMN might be the spatial domain to process mental states requiring internal representation of mental imagery with subjective experiences.

Although the listed mental states share the commonality in forming mental imagery, they are distinct from each other at a close look. For example, an autobiographical episodic memory retrieval (AEMR) state is a mental state realizing the internal representation of mental imagery remarkably. Autobiographical episodic memory has an order between episodes (scenes) abstracted from subjective experiences in past [18, 67, 68, 73]. Therefore, one can retrieve autobiographical episodic memory repeatedly and consistently. In contrast to the AEMR state, a resting state is a mental state allowing the subject to drift in subjective perspective without the order of mental imagery or the need of picturing specific contents from past experiences. As the result, the resting state consists of spontaneous mind wandering [33]. When the DMN is a set of brain regions processing the two mental states featuring internal representation, could it be possible to observe the differences between them from the dynamics of the DMN which belongs to the temporal domain? If that is the case, the functional connectivity between brain regions in the DMN might change depending on the mental states that the network executes. To test this idea, we compared the dynamics of the DMN in the two mental states.

Dynamic Functional Connectivity

Functional connectivity analysis measures the correlation between activities of two brain regions for the entire measurement duration [24]. Research on functional connectivity has defined a few brain networks with and without tasks [3, 60, 70]. At the same time, correlations in a brain network do not stay steady but change over time as cognitive activities do. Dynamic functional connectivity (DFC) is an analysis method to measure the changes in correlations between two brain regions over time [3, 17, 34]. Consequently, DFC research usually focuses on the connections of spontaneous alternations in cognitive activities to its neuronal substrates [9, 39, 58]. In this paper, we explored how two different mental states executed in the DMN could be differentiated in the dynamics of its functional connectivity.

To analyze the dynamics of a network and understand its implication, one should solve technical problems. There are two main concerns about the analysis of BOLD signals from the perspective of network analysis. One of the concerns is the high dimension of data. It implies we should consider many variables and their dependency on each other. Thus, it is hard to catch the causality of such multivariate time series signals. Further, when the connection between the observational method (fMRI BOLD) and the system under observation (neuronal substrates) is complex, it should be considered carefully to interpret observations on our hands. For DFC analysis, it has been assumed that the BOLD signals represent the neuronal activities of the brain reliably, so the concern about the observational method is resolved [21, 42]. Dimensionality reduction of a given data could resolve the remaining concern about the complexity of many variables. DFC studies analyzed correlations of every pair in the brain networks simultaneously (all-to-all) [34]. Instead of using all-to-all DFC analysis, we analyze DFC between a brain region and the other regions in the DMN, named one-to-many DFC analysis to inspect the changes in DFC for a brain region at once.

The steps of the one-to-many DFC analysis is following: We chose a brain region, the center, from the DMN and then compute DFC of the partial correlations of the center which are correlations between the center and the other brain regions in the DMN. After that, the principal component analysis was applied to the DFC of the partial correlations of the center [74]. Given the distribution of the partial correlations of the center in the DMN, the principal component analysis projects on an orthogonal basis. By that means, one can measure variances in the partial correlations of the center in orthogonal directions. We compare the directions of principal components of the partial correlations of DMN in the same and distinct mental states. If the DMN adjusts itself depending on mental states, we could observe differences in principal components for the distinct mental states. Likewise, the principal components for the same mental states would be congruent. We tested this hypothesis with an fMRI BOLD signal collected from a late blind subject.

Mental Imagery of the Blind

Because of the advanced visual system of humans, it is reckoned that visual stimuli dominate sensory inputs [35] and is closely related to mental imagery [50]. Consequently, researchers have widely investigated the relationship between mental imagery and visual impairment to learn the mechanism of mental imagery [16]. The visual sensory input is spontaneous, and its sensory field is wide so that humans mainly rely on it to navigate spaces [41, 59, 64]. Some research on blind people shows that congenitally and late blind people can perform spatial navigation tasks as much as blindfolded sighted people can do, although they are visually impaired [59, 65]. At the same time, it found differences between the blind and the sighted people also. The size of sensory fields for auditory and tactile perception is smaller than those of the visual field. Hence, auditory and tactile perceptions contain local information and are naturally serial [2, 43, 56]. Contrastingly, the visual field offers global and local information simultaneously [47]. Such a difference in sensory inputs leads blind people who prefer to employ the auditory and tactile perceptions to process mental imagery through relative locations of objects in series [37, 48, 49, 69]. Accordingly, research on serial memory of the blind shows that blind people could perform serial memory tasks better than sighted people do [4, 51, 55, 56]. It might reflect their familiarity with the serial process. In addition to that, in the case of the late blind people, activities of the visual cortex, including the primary visual cortex and the medial temporal lobe, were observed from mental imagery tasks [4, 11, 27, 54]. It implies that the late blind people can transfer the local and serial sensory inputs into global visual imagery. In short, they have advanced auditory and tactile perceptions contributing to local information and visual memory capturing a global structure of scenes by transferring local information into global visual imagery.

Concerning these facts, we assume that the late blind people have the advantage of having vivid mental imagery. In our study, we compared the dynamics of neuronal activities at the network level with a single case study of a late blind subject in two mental states, an autobiographical episodic memory retrieval state, and a resting state. Following the ample studies on the late blind people summarized above, they have an advanced ability to retrieve serial memory fluently using vivid mental imagery that is closely related to episodic memory retrieval ability. Therefore, studying a late blind subject might facilitate catching the differences in the dynamics of neuronal activities of the two mental states: the episodic memory retrieval state and the resting state. Furthermore, a late blind female subject aged 78 (called B.L.) who participated in this experiment previously attended a study showed that she could visualize vividly her episodic memory [72]. We collected the fMRI BOLD signals during two mental states and analyzed dynamic functional connectivity in the DMN using the one-to-many DFC analysis. The one-to-many DFC analysis compared the major principal components of dynamic functional connectivity in the DMN calculated from the same mental state, three times the AEMR state, and different mental states, three times the AEMR state versus a resting state.

2 Material and Method

2.1 Experiment

B.L has been blind for more than 50 years and had no known brain damage or neuronal diseases at the time she attended the experiment. She used the Braille system. We asked the subject to retrieve her morning routine which is a type of autobiographical episodic memory. First, the subject described her morning routine verbally, then she repeated it three times in silence. After the behavioral experiment, the fMRI BOLD signals of the subject were collected while she was retrieving her morning routine and resting. The study was approved by the local ethics committee of the University of Munich.

Behavior

Before an fMRI session, the subject verbally described her morning routine and the description was recorded as an audio file. After the verbal statement, she retrieved the same morning routine three times in silence. The subject cued the beginning and the end of task performance verbally. An experimenter recorded the duration of each trial based on the cue.

fMRI

We scanned the T1-weighted structural image with high resolution then the EPI sequences functional images. A foam cushion was used to minimize the effect of head movement. In the first fMRI run, B.L was asked to rest without focusing on any specific thoughts or mental imagery. After the resting state run, she repeated the retrieval of her morning routine three times, and a short pause (less than a minute) was given in between fMRI runs. An experimenter cued the beginning and end of each run. The subject listened to the cue through a speaker in the MRI room. All four runs were 7 minutes 40 seconds following the result of the behavioral experiment. Imaging was performed with a 3T MRI clinical scanner (Phillips Healthcare, Ingenia). A T1-weighted 3D structural image was acquired in sagittal orientation. Its arrangements are as follows: repetition time (TR) = 8.2 ms, echo time (TE) = 3.76 ms, flip angle (FA) = 8°, number of slices = 220, matrix = 256 x 256, 1mm isotropic voxel size. Functional images were acquired after the T1-weighted anatomical reference scan using an echo-planar image (EPI) sequence. Its arrangements are as follows: repetition time (TR) = 2.5 s, echo time (TE) = 30 ms, flip angle (FA) = 90°, number of slices = 48, number of volumes = 180, matrix = 144 x 144, 3 mm isotropic voxel size, ascending sequential acquisition in axial orientation.

2.2 Analysis

Data Preprocessing

Acquired T1-weighted anatomical images and EPI sequences were preprocessed by the default pre-processing pipeline of the CONN toolbox (www.nitrc.org/projects/conn,

RRID: SCR 009550), which is a toolbox for SPM 12 (https://www.fil.ion.ucl.ac.uk/spm/software/spm12/). The first six functional images were discarded, and 174 functional images (7 minutes 15 seconds) were used for further analysis. The preprocessing pipeline includes the realignment and unwrap, slice timing correction, outlier detection using ART (http://web.mit.edu/swg/software.
htm), direct segmentation, normalization to MNI space, and functional smoothing. Realignment and unwrap were done to the first scan using b-spline interpolation. Slice timing correction was done to match the slice at each TR/2. Images showing their frame-wise displacement above 0.9mm due to head motion or the deviation of the global BOLD signal above five standard deviations were marked as outliers and scrubbed. Segmented functional and structural data were normalized to MNI space with 1 mm and 2 mm isotropic voxels respectively using 4th order spline interpolation. Functional smoothing was done with a Gaussian kernel of 6mm full width half maximum. To remove the slow physiological noises, the high pass filter with a 0.008 Hz threshold was applied.

Regions of Interest

We employed group ICA of CONN toolbox and defined the DMN of the subject from the four trials. First, fast ICA with G1 contrast function abstracted the 40 spatial independent components after dimensionality reduction (dimension=64) [15, 36]. We picked one of the components as the DMN by comparing spatial correlation and spatial overlap to the predefined DMN offered in CONN toolbox. The predefined DMN is defined with ICA of the resting state data (n=497) of the Human Connectome Project [40]. The chosen independent spatial component contained the left and right angular gyrus (AG), the left and right parahippocampal cortex (PHC), the retrosplenial cortex (RSC), the precuneus (PRC), and a minor part of the posterior cingulate cortex (PCC) representing the posterior subsystem of the DMN. Additionally, we selected one more independent spatial component that could be regarded as the anterior subsystem or the midline core subsystem of the DMN mainly consisting of the PCC and the mPFC. Research on the DMN found that the DMN consists of a few subnetworks that may alter in number or appearance dependent on the study design and analysis methods [6, 19, 20, 45]. For that reason, we chose eight brain regions from two independent components in our study (Figure 1). We extracted ROI marks of the PCC and the mPFC from an independent component with a threshold z-score ≥ 3, and the rest in another independent component with a threshold z-score ≥ 4 except for the L/R PHC using CONN toolbox. We chose a threshold of the z-score for the L PHC and R PHC as 2.5 to include a nontrivial number of voxels (Table 1).

One-to-many Dynamic Functional Connectivity

Conventional DFC studies analyze the variance of correlations between all brain regions in a brain network (all-to-all DFC) [34]. For a brain network with n brain regions, one should consider $n(n-1)/2$ correlations simultaneously. One major drawback of this approach is the high number of variables. To find regularity in the DFC of brain networks, many researchers have hired various multivariate time series analyses using pattern recognition algorithms mainly [3, 52]. Results of such pattern recognition analysis are useful to observe brain activity per se, whereas the systematic causality between an observed pattern and its neuronal substrate

is obscure in many cases due to the complexity of the data. We suggest a new analysis method in this paper to overcome this shortage by simplifying our point of view on brain networks. The One-to-many DFC analysis considers only correlations between a chosen brain region and its connection to other brain regions in the same brain network that we call the partial correlations of the center (Figure 2). In the present study, the center means the chosen brain region of the one-to-many DFC analysis. The major advantage of the one-to-many DFC analysis is that it needs only $n - 1$ correlations or the partial correlations of the center to define the dynamics of the network. Now, the question of this study is as follows: how is the partial correlations of the center for the given measurement duration distributed in Euclidean space? One of the most well-known tools for assessing multivariate time series data in Euclidean space is the principal component analysis (PCA). When we apply the PCA to the time series of the partial correlations of the center in a brain network, then it defines a set orthogonal basis called principal components that is calculated from variances of $n - 1$ correlations over time. The first principal component is the direction in which the largest load of variance lies. The second-largest load of variance lies in the second principal component that is orthogonal to the first principal component. The biggest advantage of using PCA is the first few principal components explain the most variance of the multivariable system. If the first or the second principal components from the three trials of the AEMR state are congruent, then one can say that the partial correlations of the center in the DMN for the given duration have high similarity in direction encoding their major variance. On the contrary, one expects that the first or the second principal components from the three AEMR trials and a resting state trial are incongruent when the dynamics of the DMN adapt themselves depending on the mental states that it processes.

The congruence of principal components from the four fMRI trials (three AEMR trials and a resting state trial) can be depicted as angles between them [26, 38]. Loadings of a principal component, L, indicate the weights of variables of the data to the principal component. Hence in our case, loadings of principal components mean the weights of correlations to the center of the DMN. Let us call the first principal component of a center C from a trial A is A_1. Then $A_1 = A_1(L_{11},...,L_{17})$ means that the L_{1i} amount of contribution for $i = 1, \ldots, 7$, or weight from the correlation between C and the brain region i to the A_1. When B_1 is a first principal component of a trial B of the center C, the angle $\theta_{A,B}$ ($0 \leq \theta_{A,B} \leq \frac{\pi}{2}$) between two principal components is calculated as $\theta_{A,B} = \cos^{-1}(A_1 \cdot B_1)$ when $A_1 \cdot B_1$ is the inner product of A_1 and B_1 (the norm of A_1 and B_1 is 1). The angle $\theta_{A,B}$ tells how parallel, or in other words, how similar the directions of the first principal components of trial A and trial B. Similar methods to define congruence of principal components from different group suggested previously [38, 76]. When one of the first two principal components of trial A is aligned parallel to that of trial B i.e., $\theta_{A,B}$ is close to zero degree, the weight of each correlation is similar in both trials. If the angle between chosen principal components is close to 90 degrees, then the weights of the principal components are largely dissimilar. As the result, we expect to see the small angles (close to 0 degree) between chosen principal components of the partial correlations of the identical center from three AEMR trials. Further, the big angles (close to 90 degrees) between these principal components

and the first or second principal component of the partial correlations of the center from a resting-state, if the DFC of the DMN measured with the partial correlations of the center adapts itself depending on mental states.

In this study, we employed the Pearson correlation coefficient to calculate the bidirectional and linear correlation between two brain regions and the sliding window method with the window width of 10 consecutive images (=25 sec with TR=2.5 sec). The weight of the window is constant so that the window has a rectangular shape. The window slides an image per step; therefore, 165-time points for 174 preprocessed images described the variance in partial correlations. Given distributions of partial correlations of the center, we applied the PCA to the partial correlations of the center for four trials (three AEMR trials and one resting-state trial). Before application of the PCA, we aligned the data to have the zero mean. We calculated angles between the first, the second and the third principal components of four trials, then picked only one principal component from each trial having a smaller angle to principal components from other trials. We repeated the same analysis by choosing every brain region in the DMN as the center at a time.

3 Results

Behavior

B.L reported that she could retrieve the same morning routine in detail for the retrieval trials outside of the MRI machine and inside of the machine. The subject described her morning routine as a sequence of episodes. The term 'episode' is used here to refer to an event that happened in a specific location. Between episodes, navigational descriptions to move to the next location appeared. As an example, a scene in her bedroom is as follows:

> "I imagined lying in bed having just woken up. I then put my feet to the left, as usual. Out of the bed, got the shoes, that were right there. Get up. Making my way around the bed, then there is the door. Through the door into the corridor. To the right and immediately to the left again, there is the toilet, something one needs in the morning."

In the verbal statement, retrieval in silence, and trials in an MRI machine, she reported that the last scene of her morning routine was that she is waiting for her husband sitting at the breakfast table in the living room. 7 minutes 40 seconds was the mean of measured time for the three retrieval trials in silence (SD < 10 sec).

fMRI

The first three principal components of four trials explain over 80% of the entire variance in the DMN for each chosen center. Criteria for selecting a principal component from a trial were as follows: we computed angles between the first three principal components of the three AEMR trials one by one, i.e., $\theta_{AB}(i,j)= (PC_A(i),PC_B(j))$ for A, B = 1,2,3 and i, j = 1,2,3 is the angle between ith and jth principal components of a trial A and a trial B respectively. Then we chose $PC_A(i)$ having the smallest angle to $PC_B(j)$ for $A \neq B$. For the resting state trial, we chose the principal component having smallest angle to the chosen principal components of three AEMR trials. When a $PC_A(i)$ has the smallest angle to a chosen principal component of a trial B and $PC_A(j)$ for $i \neq j$ has the smallest angle to the chosen principal components of another trial, then we chose the principal components giving the smaller mean of three angles between the AEMR trials. The same holds for the choice of a principal component of the resting state trial. As shown in Table 2, the first principal components showed the smallest angles between them except for the left and right AG and the RSC. Table 3 showed the angles between the chosen principal components. To assess the similarity between the principal components of three AEMR trials and the resting state trial, the ratio of the mean angles between the chosen principal components of three AEMR trials to that of all four trials of each center was computed (Table 4). The implication of the ratio is as follows: the chosen principal components from four trials are aligned in the same direction when the ratio is close to 1. The chosen principal components of three AEMR trials align in the same direction, but it differs from the direction of that of the resting state trial when the ratio is smaller than 1; the smaller is the more distinct. The chosen principal components of the three AEMR trials align in the

direction of the resting state trial than they do between themselves when the ratio is bigger than 1.

The result, as shown in Table 4, principal components from correlations of the PCC center had the smallest mean angle (13.05 degrees) between three AEMR trials. In addition, its ratio to the mean angle of four trials (0.67) was the smallest compared to the ratios of the other centers (Table 4). The small angles between the first principal components of three AMER trials indicate that the weights of correlations to the variances in partial correlations between the PCC and other brain regions in the DMN stayed consistent for the AMER trials. Furthermore, the ratio between the mean angle from the AEMR trials and the mean angle together with the resting state trial suggested that the weights of correlations modified depending on a mental state processed in the DMN. In Figure 3, distinctions in loadings of correlations are presented. The chief distinction between the AEMR trials and the resting state trial in the loadings of their chosen principal components of the PCC center was observed in the weight of R PHC - PCC correlation.

The chosen principal components from correlations of the mPFC center also had the relatively small mean angle between three AEMR trials (13.91 degrees). However, in contrast to the case of the PCC, its ratio (0.88) to the mean angle together with the resting state trial was relatively large. This result implies that the weights of correlations of the mPFC were similar for both mental states. For the case of the R PHC center, the ratio between mean angles is relatively small (0.71). Nevertheless, the mean angle between the chosen principal components of the AEMR trials (23.15 degrees) is almost twice larger as that of the PCC center case. Except for the PCC, the mPFC, and the right PHC center, other brain regions did not show the high similarity between the chosen principal components of the three AEMR trials nor their distinct dissimilarity to that of the resting state trial.

4 Discussion

In this exploratory study, we aimed to investigate adaptations in the DFC of the DMN in two mental states with a new analysis method called the one-to-many DFC. For this purpose, we chose the two mental states, the AEMR state and the resting state, and conducted behavioral and fMRI experiments with a blind subject who has an advanced ability to envisage mental imagery. Given the verbal description of the morning routine, we could see that the spatial navigation guided the streaming of episodes. In the behavioral experiment in silence, the subject could retrieve the morning routine with a constant retrieval duration for each trial. These results from behavioral experiments imply that there is regularity in dynamics of the DMN to retrieve the morning routine, which is a distinctive feature of the AEMR state compared to the resting state. In the further fMRI experiment, the dynamics of the DMN in the AEMR state and the resting state were analyzed by one-to-many DFC analysis. The new analysis method measured only the partial correlations of the center in the DMN at once, then computed an orthonormal basis of the variance in the partial correlations with PCA. The most

parallelly aligned principal component among the first three principal components of each trial was chosen by measuring the angle between them. In the case of the three AEMR trials, their first principal components had the smallest angles between them regardless of the choice of the center. The mean angles between the chosen principal components showed that the principal components of the PCC center align with each other most closely (13.05 degrees) compared to the results from the other centers (Table 4). This result implied that the dynamics of the DMN in the AEMR state analyzed via the PCC center were most consistent for the three AEMR trials. At the same time, we computed changes in the mean angle when the chosen principal component of the resting state trial was included. The result suggested that the selected principal components of the three AEMR trials align with that of the resting state in the most distinct direction when the PCC is the center (AEMR/Resting = 0.67), compared to the results from the other centers (Table 4). Previous fMRI studies on the DMN showed that the PCC is the most reliable marker in the adaptation of the DMN with block designs using self-referential stimuli [20, 75]. In our study, we could show consistent results by hiring a subject-driven experimental paradigm without external cues for time control [60]. Furthermore, we could show the congruent dynamics of AEMR states and their distinction from that of the resting state by the One-to-many DFC analysis. To sum up the results of our study, the dynamics of the DMN adapted themselves depending on the mental state, and it was possible to observe such adaptations via partial functional connectivity of the PCC in the DMN using one-to-many DFC analysis.

Interestingly, the PCC is a well-known functional and structural hub of the brain networks [1, 13, 30, 32, 66]. To date, several studies on the brain network have speculated that hubs in human brains boost efficient communication between brain regions [8, 14, 57, 70]. Following the idea of hubs of brain networks, it is reasonable to expect to see that connections between brain regions in a local brain network adapt themselves depending on a mental state processed in the network via its hubs. Correspondingly, the results of the one-to-many DFC analysis on the DMN demonstrated that the DMN adjusts itself via the PCC depending on the mental state. By contrast, the analysis results of the mPFC center, which is also one of the known functional and structural hubs of the brain, did not demonstrate the distinctive dynamics of two mental states in the DMN (AEMR/Resting = 0.88) compared to the PCC center case. It can therefore be assumed that the local hub of the DMN mediating adjustment within the network is the PCC, but not the mPFC. Consistent with the implication, the anatomical and structural connections between the PCC and the other brain regions in the DMN are confirmed by cytoarchitecture and diffusion tensor imaging [29, 71].

Besides the results of the PCC, the R PHC demonstrated that its dynamics for two mental states were relatively discriminated, which are represented by the small ratio between mean angles (AEMR/Resting = 0.71). Unlike the PCC and the mPFC, the R PHC is not one of the hubs in brain networks. As one would expect, the chosen principal components of three AEMR trials of the R PHC center aligned in less coherent directions (23.15 degrees) compared to that of the PCC (13.05 degrees) and the mPFC (13.91 degrees). Even though it did not show

high coherence in the AEMR state, the distinction in the dynamics of the DMN in the two mental states was relatively large (AEMR/Resting = 0.71). It could be explained by the fact that the connection between the PCC and the R PHC varied considerably for the two mental states we examined. As the loadings of each correlation to the chosen principal components of the PCC center suggested in Figure 4, the loading of the R PHC to the PCC center varied around twice bigger than that of the other regions of the PCC. An implication of this result is that the functional connectivity between the PCC and the R PHC takes a pivotal role in explaining the difference between the two mental states in the current study. One of the known functions of the PHC is the recognition of local scenes and contextual association [5, 22, 44]. Accordingly, the activity of the PHC might be the key to retrieving coherent mental imagery of scenes, in contrast to the resting state which does not require such a function. Moreover, studies on the lateralization of the medial temporal lobe (MTL) have suggested that the right MTL is related to spatial navigation, in contrast to the lateralized activity of the left MTL in context dependent memory encoding tasks [25, 46, 61]. As a consequence of the result from the one-to-many DFC analysis together with the verbal statement, spatial navigation in mental imagery of the subject might drive the adaptation of the functional connectivity between the R PHC and the PCC in the DMN in the current study.

5 Limit

However, being limited to a single subject, this study lacks generality. This study takes a single subject who is blind having a specifically advanced ability to perform mental imagery tasks. To provide generalizable evidence, we conducted a group study of the sighted subjects, and its result is in preparation for publication.

6 Conclusion

The adaptation of dynamics in brain networks is believed that it reflects the streaming of mental states, which is the nature of humans. The one-to-many DFC analysis may offer us a better understanding of the adjustment of brain dynamics at the local network level using a simple analysis method and subject-driven mental states. Furthermore, the one-to-many DFC analysis would be an intriguing analysis method that could suggest specific targets for neuronal circuit studies within a local brain network.

Disclosure of conflict of interest

The authors declare that there are no conflicts of interest.

Data Availability Statement

The data that support the findings of this study are available on request from the corresponding author. The data are not publicly available due to privacy or ethical restrictions.

Acknowledgement

We thank Isolde Zondler and Dr. Urs Zondler for their donation to support this research project.

References

[1] Sophie Achard, Raymond Salvador, Brandon Whitcher, John Suckling, and ED Bullmore. A resilient, low-frequency, small-world human brain functional network with highly connected association cortical hubs. *Journal of Neuroscience*, 26(1):63–72, 2006.

[2] Claude Alain, Stephen R Arnott, Stephanie Hevenor, Simon Graham, and Cheryl L Grady. "what" and "where" in the human auditory system. *Proceedings of the national academy of sciences*, 98(21):12301–12306, 2001.

[3] Elena A Allen, Eswar Damaraju, Sergey M Plis, Erik B Erhardt, Tom Eichele, and Vince D Calhoun. Tracking whole-brain connectivity dynamics in the resting state. *Cerebral cortex*, 24(3):663–676, 2014.

[4] Amir Amedi, Noa Raz, Pazit Pianka, Rafael Malach, and Ehud Zohary. Early 'visual'cortex activation correlates with superior verbal memory performance in the blind. *Nature neuroscience*, 6(7):758–766, 2003.

[5] Elissa M Aminoff, Kestutis Kveraga, and Moshe Bar. The role of the parahippocampal cortex in cognition. *Trends in cognitive sciences*, 17(8):379–390, 2013.

[6] Jessica R Andrews-Hanna, Jay S Reidler, Jorge Sepulcre, Renee Poulin, and Randy L Buckner. Functional-anatomic fractionation of the brain's default network. *Neuron*, 65(4):550–562, 2010.

[7] Jessica R Andrews-Hanna, Jonathan Smallwood, and R Nathan Spreng. The default network and self-generated thought: Component processes, dynamic control, and clinical relevance. *Annals of the New York Academy of Sciences*, 1316(1):29–52, 2014.

[8] Danielle S Bassett, Andreas Meyer-Lindenberg, Sophie Achard, Thomas Duke, and Edward Bullmore. Adaptive reconfiguration of fractal small-world human brain functional networks. *Proceedings of the National Academy of Sciences*, 103(51):19518–19523, 2006.

[9] Danielle S Bassett, Nicholas F Wymbs, Mason A Porter, Peter J Mucha, Jean M Carlson, and Scott T Grafton. Dynamic reconfiguration of human brain networks during learning. *Proceedings of the National Academy of Sciences*, 108(18):7641– 7646, 2011.

[10] Bharat Biswal, F Zerrin Yetkin, Victor M Haughton, and James S Hyde. Functional connectivity in the motor cortex of resting human brain using echo-planar mri. *Magnetic resonance in medicine*, 34(4):537–541, 1995.

[11] Holly Bridge, Stephen Harrold, Emily A Holmes, Mark Stokes, and Christopher Kennard. Vivid visual mental imagery in the absence of the primary visual cortex. *Journal of neurology*, 259(6):1062–1070, 2012.

[12] Randy L Buckner and Daniel C Carroll. Self-projection and the brain. *Trends in cognitive sciences*, 11(2):49–57, 2007.

[13] Randy L Buckner, Jorge Sepulcre, Tanveer Talukdar, Fenna M Krienen, Hesheng Liu, Trey Hedden, Jessica R Andrews-Hanna, Reisa A Sperling, and Keith A Johnson. Cortical hubs revealed by intrinsic functional connectivity: mapping, assessment of stability, and relation to alzheimer's disease. *Journal of neuroscience*, 29(6):1860–1873, 2009.

[14] Ed Bullmore and Olaf Sporns. Complex brain networks: graph theoretical analysis of structural and functional systems. *Nature reviews neuroscience*, 10(3):186–198, 2009.

[15] Vince D Calhoun, Tulay Adali, Godfrey D Pearlson, and James J Pekar. A method for making group inferences from functional mri data using independent component analysis. *Human brain mapping*, 14(3):140–151, 2001.

[16] Zaira Cattaneo, Tomaso Vecchi, Cesare Cornoldi, Irene Mammarella, Daniela Bonino, Emiliano Ricciardi, and Pietro Pietrini. Imagery and spatial processes in blindness and visual impairment. *Neuroscience & Biobehavioral Reviews*, 32(8):1346–1360, 2008.

[17] Catie Chang and Gary H Glover. Time–frequency dynamics of resting-state brain connectivity measured with fmri. *Neuroimage*, 50(1):81–98, 2010.

[18] Martin A Conway. Autobiographical memory. In *Memory*, pages 165–194. Elsevier, 1996.

[19] Jessica S Damoiseaux, SARB Rombouts, Frederik Barkhof, Philip Scheltens, Cornelis J Stam, Stephen M Smith, and Christian F Beckmann. Consistent resting-state networks across healthy subjects. *Proceedings of the national academy of sciences*, 103(37):13848–13853, 2006.

[20] Christopher G Davey, Jesus Pujol, and Ben J Harrison. Mapping the self in the brain's default mode network. *Neuroimage*, 132:390–397, 2016.

[21] Gustavo Deco, Viktor K Jirsa, and Anthony R McIntosh. Emerging concepts for the dynamical organization of resting-state activity in the brain. *Nature Reviews Neuroscience*, 12(1):43–56, 2011.

[22] Russell A Epstein. Parahippocampal and retrosplenial contributions to human spatial navigation. *Trends in cognitive sciences*, 12(10):388–396, 2008.

[23] Michael D Fox, Abraham Z Snyder, Justin L Vincent, Maurizio Corbetta, David C Van Essen, and Marcus E Raichle. The human brain is intrinsically organized into dynamic, anticorrelated functional networks. *Proceedings of the National Academy of Sciences*, 102(27):9673–9678, 2005.

[24] Karl J Friston, Chris D Frith, Peter F Liddle, and Richard SJ Frackowiak. Functional connectivity: the principal-component analysis of large (pet) data sets. *Journal of Cerebral Blood Flow & Metabolism*, 13(1):5–14, 1993.

[25] Alexandra J Golby, Russell A Poldrack, James B Brewer, David Spencer, John E Desmond, Arthur P Aron, and John DE Gabrieli. Material-specific lateralization in the medial temporal lobe and prefrontal cortex during memory encoding. *Brain*, 124(9):1841–1854, 2001.

[26] John C Gower. Multivariate analysis and multidimensional geometry. *Journal of the Royal Statistical Society: Series D (The Statistician)*, 17(1):13–28, 1967.

[27] Manu S Goyal, Peter J Hansen, and Colin B Blakemore. Tactile perception recruits functionally related visual areas in the late-blind. *Neuroreport*, 17(13):1381–1384, 2006.

[28] Michael D Greicius, Ben Krasnow, Allan L Reiss, and Vinod Menon. Functional connectivity in the resting brain: a network analysis of the default mode hypothesis. *Proceedings of the National Academy of Sciences*, 100(1):253–258, 2003.

[29] Michael D Greicius, Kaustubh Supekar, Vinod Menon, and Robert F Dougherty. Resting-state functional connectivity reflects structural connectivity in the default mode network. *Cerebral cortex*, 19(1):72–78, 2009.

[30] Patric Hagmann, Leila Cammoun, Xavier Gigandet, Reto Meuli, Christopher J Honey, Van J Wedeen, and Olaf Sporns. Mapping the structural core of human cerebral cortex. *PLoS biology*, 6(7):e159, 2008.

[31] Demis Hassabis and Eleanor A Maguire. Deconstructing episodic memory with construction. *Trends in cognitive sciences*, 11(7):299–306, 2007.

[32] Christopher J Honey, Rolf K¨otter, Michael Breakspear, and Olaf Sporns. Network structure of cerebral cortex shapes functional connectivity on multiple time scales. *Proceedings of the National Academy of Sciences*, 104(24):10240–10245, 2007.

[33] Russell T Hurlburt, Ben Alderson-Day, Charles Fernyhough, and Simone Ku¨hn. What goes on in the resting-state? a qualitative glimpse into resting-state experience in the scanner. *Frontiers in psychology*, 6:1535, 2015.

[34] R Matthew Hutchison, Thilo Womelsdorf, Elena A Allen, Peter A Bandettini, Vince D Calhoun, Maurizio Corbetta, Stefania Della Penna, Jeff H Duyn, Gary H Glover, Javier Gonzalez-Castillo, et al. Dynamic functional connectivity: promise, issues, and interpretations. *Neuroimage*, 80:360–378, 2013.

[35] Fabian Hutmacher. Why is there so much more research on vision than on any other sensory modality? *Frontiers in psychology*, page 2246, 2019.

[36] Aapo Hyvarinen. Fast and robust fixed-point algorithms for independent component analysis. *IEEE transactions on Neural Networks*, 10(3):626–634, 1999.

[37] Tina Iachini, Gennaro Ruggiero, and Francesco Ruotolo. Does blindness affect egocentric and allocentric frames of reference in small and large scale spaces? *Behavioural brain research*, 273:73–81, 2014.

[38] WJ Krzanowski. Between-groups comparison of principal components. *Journal of the American Statistical Association*, 74(367):703–707, 1979.

[39] Aaron Kucyi and Karen D Davis. Dynamic functional connectivity of the default mode network tracks daydreaming. *Neuroimage*, 100:471–480, 2014.

[40] Guenther Lab. Boston university college of health & rehabilitation sciences: Sargent colleg guenther lab & functional connectivity analyses, April 2017. Accessed: 202204-01.

[41] Barbara Landau, Henry Gleitman, and Elizabeth Spelke. Spatial knowledge and geometric representation in a child blind from birth. *Science*, 213(4513):1275–1278, 1981.

[42] Nikos K Logothetis. What we can do and what we cannot do with fmri. *Nature*, 453(7197):869–878, 2008.

[43] Jack M Loomis, Roberta L Klatzky, and Susan J Lederman. Similarity of tactual and visual picture recognition with limited field of view. *Perception*, 20(2):167–177, 1991.

[44] Eleanor A Maguire, CD Frith, N Burgess, JG Donnett, and J O'keefe. Knowing where things are: Parahippocampal involvement in encoding object locations in virtual large-scale space. *Journal of cognitive neuroscience*, 10(1):61–76, 1998.

[45] Lorenzo Mancuso, Sara Cavuoti-Cabanillas, Donato Liloia, Jordi Manuello, Giulia Buzi, Franco Cauda, and Tommaso Costa. Tasks activating the default mode network map multiple functional systems. *Brain Structure and Function*, 227(5):1711– 1734, 2022.

[46] Jonathan Miller, Andrew J Watrous, Melina Tsitsiklis, Sang Ah Lee, Sameer A Sheth, Catherine A Schevon, Elliot H Smith, Michael R Sperling, Ashwini Sharan, Ali Akbar Asadi-Pooya, et al. Lateralized hippocampal oscillations underlie distinct aspects of human spatial memory and navigation. *Nature communications*, 9(1):1– 12, 2018.

[47] Fiona N Newell, Andrew T Woods, Marion Mernagh, and Heinrich H Bu¨lthoff. Visual, haptic and crossmodal recognition of scenes. *Experimental Brain Research*, 161(2):233–242, 2005.

[48] Matthijs L Noordzij, Sander Zuidhoek, and Albert Postma. The influence of visual experience on the ability to form spatial mental models based on route and survey descriptions. *Cognition*, 100(2):321–342, 2006.

[49] Achille Pasqualotto, Mary Jane Spiller, Ashok S Jansari, and Michael J Proulx. Visual experience facilitates allocentric spatial representation. *Behavioural Brain Research*, 236:175–179, 2013.

[50] Joel Pearson, Thomas Naselaris, Emily A Holmes, and Stephen M Kosslyn. Mental imagery: functional mechanisms and clinical applications. *Trends in cognitive sciences*, 19(10):590–602, 2015.

[51] Albert Postma, Sander Zuidhoek, Matthijs L Noordzij, and Astrid ML Kappers. Differences between early-blind, late-blind, and blindfolded-sighted people in haptic spatial-configuration learning and resulting memory traces. *Perception*, 36(8):1253–1265, 2007.

[52] Maria Giulia Preti, Thomas AW Bolton, and Dimitri Van De Ville. The dynamic functional connectome: State-of-the-art and perspectives. *Neuroimage*, 160:41–54, 2017.

[53] Marcus E Raichle, Ann Mary MacLeod, Abraham Z Snyder, William J Powers, Debra A Gusnard, and Gordon L Shulman. A default mode of brain function. *Proceedings of the National Academy of Sciences*, 98(2):676–682, 2001.

[54] Noa Raz, Amir Amedi, and Ehud Zohary. V1 activation in congenitally blind humans is associated with episodic retrieval. *Cerebral Cortex*, 15(9):1459–1468, 2005.

[55] Noa Raz, Ella Striem, Golan Pundak, Tanya Orlov, and Ehud Zohary. Superior serial memory in the blind: a case of cognitive compensatory adjustment. *Current Biology*, 17(13):1129–1133, 2007.

[56] Brigitte R¨oder, Frank R¨osler, and Helen J Neville. Auditory memory in congenitally blind adults: a behavioral-electrophysiological investigation. *Cognitive Brain Research*, 11(2):289–303, 2001.

[57] Mikail Rubinov and Olaf Sporns. Complex network measures of brain connectivity:

uses and interpretations. *Neuroimage*, 52(3):1059–1069, 2010.

[58] Manish Saggar, Olaf Sporns, Javier Gonzalez-Castillo, Peter A Bandettini, Gunnar Carlsson, Gary Glover, and Allan L Reiss. Towards a new approach to reveal dynamical organization of the brain using topological data analysis. *Nature communications*, 9(1):1–14, 2018.

[59] Victor R Schinazi, Tyler Thrash, and Daniel-Robert Chebat. Spatial navigation by congenitally blind individuals. *Wiley Interdisciplinary Reviews: Cognitive Science*, 7(1):37–58, 2016.

[60] William R Shirer, Srikanth Ryali, Elena Rykhlevskaia, Vinod Menon, and Michael D Greicius. Decoding subject-driven cognitive states with whole-brain connectivity patterns. *Cerebral cortex*, 22(1):158–165, 2012.

[61] Hugo J Spiers, Neil Burgess, Eleanor A Maguire, Sallie A Baxendale, Tom Hartley, Pamela J Thompson, and John O'Keefe. Unilateral temporal lobectomy patients show lateralized topographical and episodic memory deficits in a virtual town. *Brain*, 124(12):2476–2489, 2001.

[62] R Nathan Spreng and Cheryl L Grady. Patterns of brain activity supporting autobiographical memory, prospection, and theory of mind, and their relationship to the default mode network. *Journal of cognitive neuroscience*, 22(6):1112–1123, 2010.

[63] R Nathan Spreng, Raymond A Mar, and Alice SN Kim. The common neural basis of autobiographical memory, prospection, navigation, theory of mind, and the default mode: a quantitative meta-analysis. *Journal of cognitive neuroscience*, 21(3):489– 510, 2009.

[64] Catherine Thinus-Blanc and Florence Gaunet. Representation of space in blind persons: vision as a spatial sense? *Psychological bulletin*, 121(1):20, 1997.

[65] Carla Tinti, Mauro Adenzato, Marco Tamietto, and Cesare Cornoldi. Visual experience is not necessary for efficient survey spatial cognition: evidence from blindness. *Quarterly journal of experimental psychology*, 59(7):1306–1328, 2006.

[66] Dardo Tomasi and Nora D Volkow. Association between functional connectivity hubs and brain networks. *Cerebral cortex*, 21(9):2003–2013, 2011.

[67] Endel Tulving. 12. episodic and semantic memory. *Organization of memory/Eds E. Tulving, W. Donaldson, NY: Academic Press*, pages 381–403, 1972.

[68] Endel Tulving. Episodic memory: From mind to brain. *Annual review of psychology*, 53(1):1–25, 2002.

[69] Simon Ungar, Mark Blades, and Christopher Spencer. Mental rotation of a tactile layout by young visually impaired children. *Perception*, 24(8):891–900, 1995.

[70] Martijn P van den Heuvel and Olaf Sporns. Network hubs in the human brain. *Trends in cognitive sciences*, 17(12):683–696, 2013.

[71] Brent A Vogt, Leslie Vogt, and Steven Laureys. Cytology and functionally correlated circuits of human posterior cingulate areas. *Neuroimage*, 29(2):452–466, 2006.

[72] Jana von Trott zu Solz, Marco Paolini, and Sarita Silveira. Does touch inhibit visual imagery? a case study on acquired blindness. *PsyCh Journal*, 6(2):139–140, 2017.

[73] Mark A Wheeler, Donald T Stuss, and Endel Tulving. Toward a theory of episodic memory: the frontal lobes and autonoetic consciousness. *Psychological bulletin*, 121(3):331, 1997.

[74] Svante Wold, Paul Geladi, Kim Esbensen, and Jerker Ohman. Multi-way principal¨ components-and pls-analysis. *Journal of chemometrics*, 1(1):41–56, 1987.

[75] Xiaoxiao Xu, Hong Yuan, and Xu Lei. Activation and connectivity within the default mode network contribute independently to future-oriented thought. *Scientific reports*, 6(1):1–10, 2016.

[76] Kiyoung Yang and Cyrus Shahabi. A pca-based similarity measure for multivariate time series. In *Proceedings of the 2nd ACM international workshop on Multimedia databases*, pages 65–74, 2004.

Table 1: MNI coordinates
Coordinates of the center for regions of interest in the MNI space.

	x,y,z	Number of Voxels
L AG	-40, -75, 22	517
R AG	40, -71, 26	510
L PHC	-29, -38, -17	86
R PHC	22, -38, -16	41
PCC	0, -53, 25	420
mPFC	0, 57, -7	847
PRC	0, -60, 42	539
RSC	2, -60, 16	765

Table 2: Chosen principal components (PC) and the amount of explained variance it explains

PC(%)	PCC	mPFC	L AG	R AG	L PHC	R PHC	PRC	RSC
AEMR1	1(66)	1(61)	1(54)	2(31)	1(43)	1(46)	1(49)	1(39)
AEMR2	1(65)	1(60)	1(50)	1(55)	2(32)	1(59)	2(24)	2(21)
AEMR3	1(51)	1(53)	1(49)	1(50)	1(37)	1(46)	2(25)	1(37)
Resting	1(62)	1(61)	2(28)	1(49)	1(65)	1(64)	1(52)	1(42)

Table 3: Angles between chosen principal components of each fMRI run

(°)	PCC	mPFC	L AG	R AG	L PHC	R PHC	PRC	RSC
AEMR1-AEMR2	8.98	12.88	49.37	33.09	25.00	20.64	35.84	48.50
AEMR2-AEMR3	16.64	15.42	10.71	18.17	49.64	30.75	29.40	52.64
AEMR3-AEMR1	13.54	13.44	44.43	48.14	34.96	18.05	31.09	10.06
Resting-AEMR1	21.80	13.25	58.80	14.39	6.53	25.58	24.83	35.41
Resting-AEMR2	22.17	19.28	13.22	45.06	22.07	44.62	34.42	52.41
Resting-AEMR3	33.58	20.26	16.83	60.55	34.01	55.70	17.73	29.97

Table 4: Mean angles between chosen principal components and the ratio between them

	PCC	mPFC	L AG	R AG	L PHC	R PHC	PRC	RSC
AEMR(°)	13.05	13.91	34.84	33.14	36.53	23.15	32.11	37.07
+ Rest(°)	19.45	15.75	32.23	36.57	28.7	32.56	28.88	38.17
Ratio	0.67	0.88	1.08	0.91	1.27	0.71	1.11	0.97

Center: the center region of the DMN, AEMR: the mean angle between principal components of three AEMR trials (Sample size = 3), +Rest: the mean angle between principal components of three AEMR and a resting state trial (Sample size = 6), Ratio: AEMR/+Rest

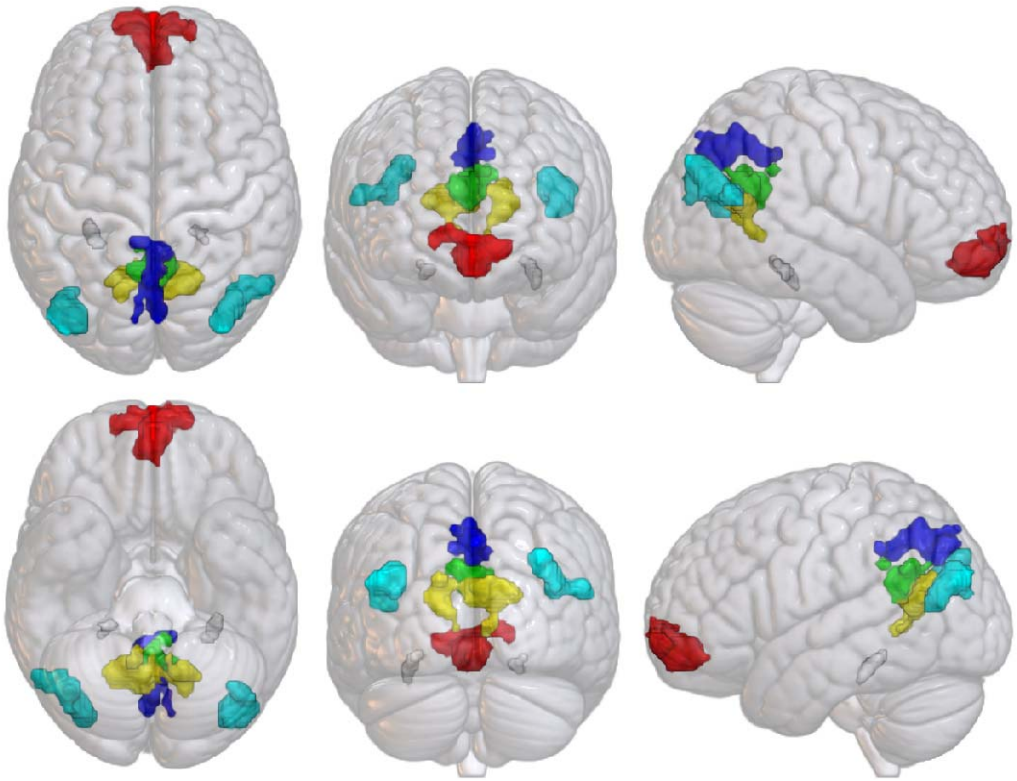

Figure 1: Regions of interest

L/R AG: Cyan, L/R PHC: White, PCC: Green, mPFC: Red, PRC: Blue, RSC: Yellow
The image was created by MRIcroGL.

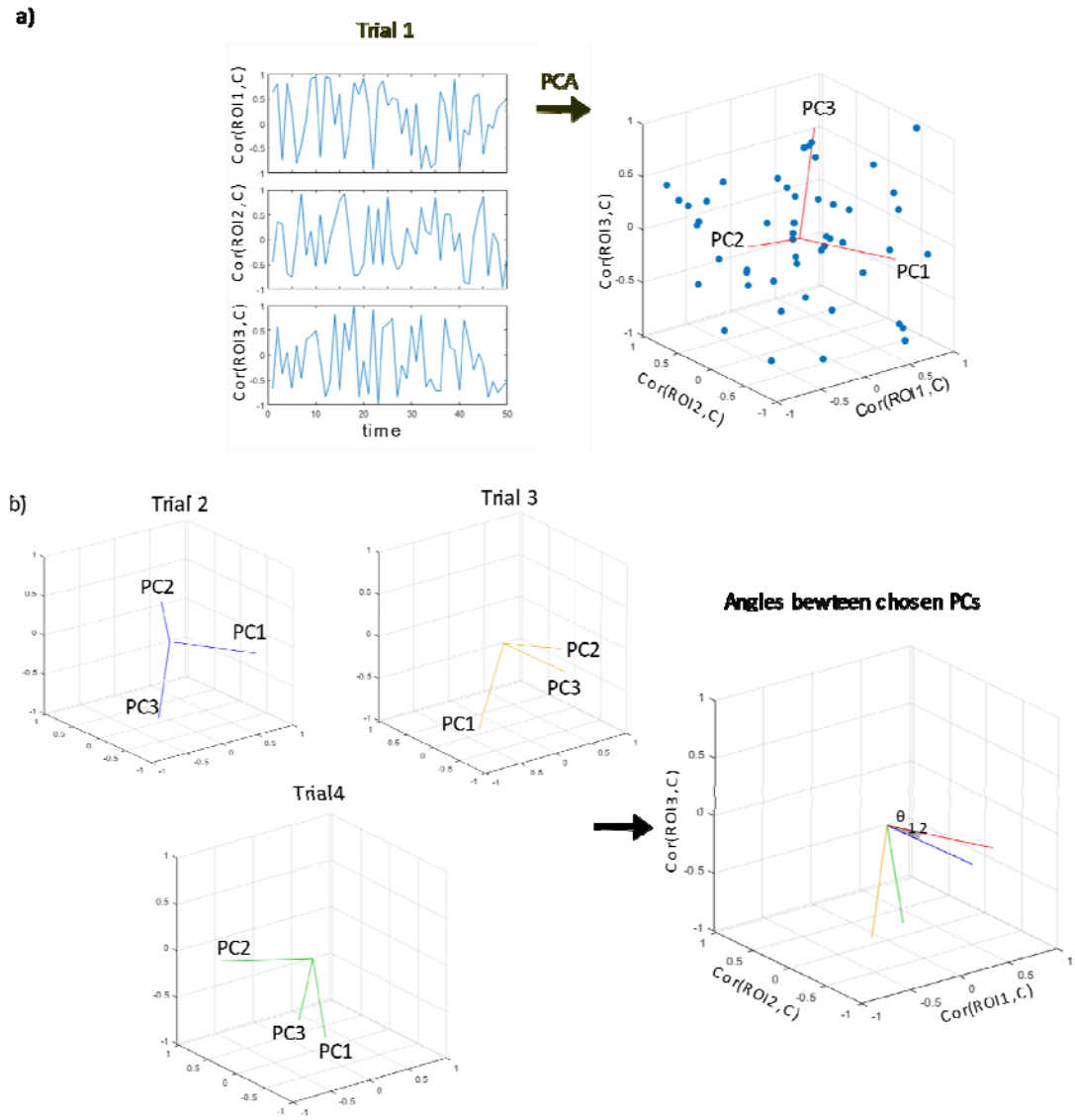

Figure 2: One-to-many dynamic functional connectivity analysis

An example with a local brain network of 4 ROIs. a) When C is the center, the correlations between C and the other three ROIs are computed using the sliding window method. The principal components (PC) of partial correlations of the C provide an orthonormal basis for the variances in the partial correlations. b) The angle between chosen principal components. For example, θ_{12} measures the congruence of the first principal components from trial 1 and trial 2.

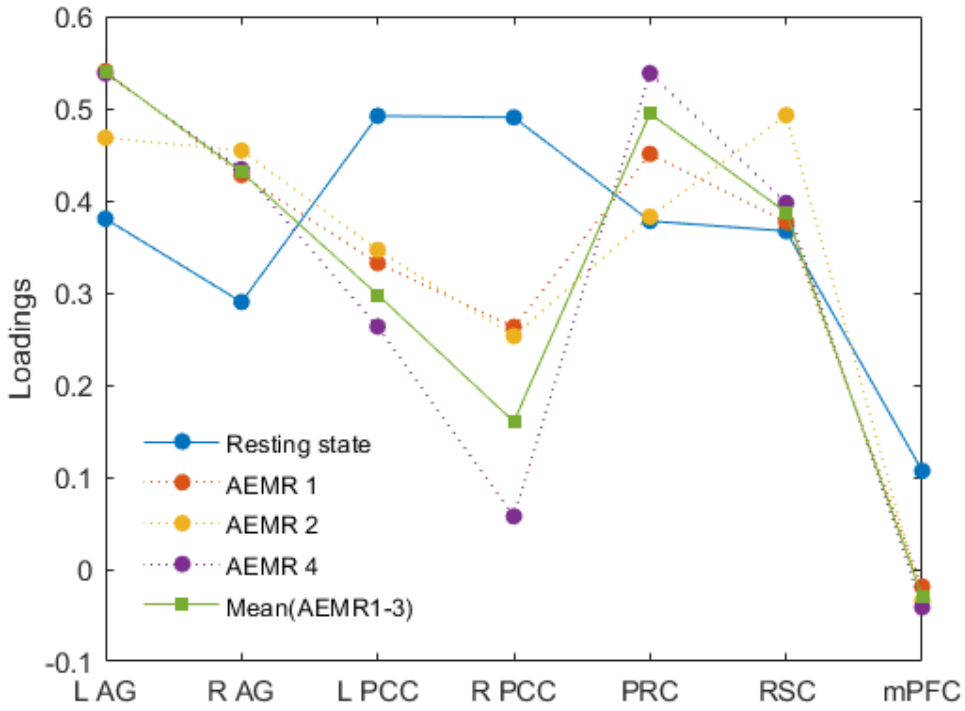

Figure 3: Loadings of the first principal components of the PCC center

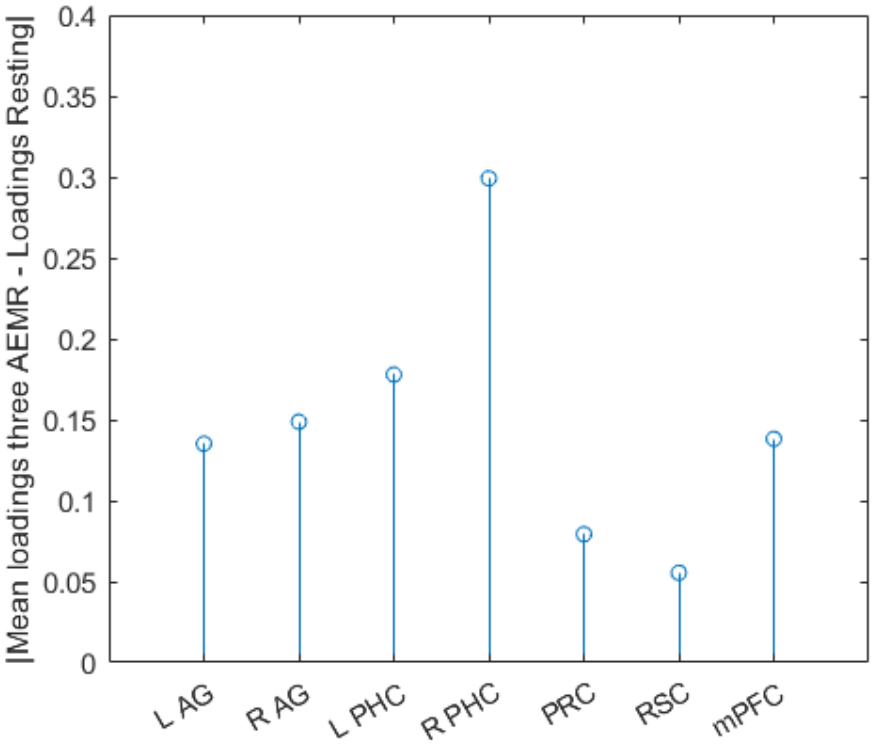

Figure 4: Difference in loadings of the first principal components of the PCC center